Photoinduced Electron-Transfer Reactions in a Chlorophyllide-Pheophorbide Cyclophane. A Model for Photosynthetic Reaction Centers

Robert E. Overfield,[†,§] Avigdor Scherz,[†] Kenneth J. Kaufmann,[†,⊥] and Michael R. Wasielewski*[‡]

Contribution from the Chemistry Division, Argonne National Laboratory, Argonne, Illinois 60439, and the Department of Chemistry, University of Illinois, Urbana, Illinois 61801. *Received November 23, 1982*

Abstract: The fluorescence and the lowest excited triplet state yields for a chlorophyllide–pheophorbide cyclophane are strongly quenched as the dielectric constant of the solvent in which it is dissolved increases. The decrease in fluorescence yield is accompanied by a decrease in fluorescence lifetime. The radiative rate for fluorescence remains approximately constant. Fluorescence decays of the cyclophane are best fit with two exponentials. The short component is 250 ± 50 ps, while the long component is about 2–4 ns. Time resolved absorbance changes at 655 and 445 nm are used to follow the decay of the excited states back to the ground state. A residual absorbance having a lifetime in excess of 30 ns is found in all solvents and is ascribed to the lowest excited triplet state of the cyclophane. After correction for this contribution the decay of the absorbance changes is best fit with a single exponential. In dichloromethane and butyronitile the absorbance decay times, 1.6 ns and 435 ps, respectively, are longer than the 250-ps fluorescence emission component of the cyclophane in these solvents. This indicates that a nonemissive excited state is formed. The observed dependence of both the fluorescence and the absorption change decays on the solvent dielectric constant suggests that quenching of the lowest excited singlet state involves an electron-transfer process. The effect of solvent dielectric constant on the quenching is analyzed in terms of the energetics of the electron-transfer reaction. The electron-transfer rate is 2×10^9 s^{-1}, while the rate of the back electron transfer yielding the cyclophane in its ground electronic state is 10^9 s^{-1}. The forward electron-transfer rate is about 100 times slower than that of photosynthetic reaction centers despite the close proximity of the donor and the acceptor (<6 Å). The difference in electron-transfer rates between the cyclophane and photosynthetic reaction centers is rationalized in terms of the importance of donor–acceptor orientation.

Electron-transfer reactions play a crucial role in many chemical and biological systems. Most electron-transfer processes that have been studied in fluid solution share the common characteristic that both the distance and the relative orientation of the electron donor with respect to the electron acceptor are unknown. These ambiguities result from the fact that the donor and acceptor must diffuse together to form an encounter complex of unknown structure prior to electron transfer. The structural features of the donor–acceptor complex that maximize the efficiency of the electron-transfer process are usually only indirectly inferred from the experiments. Ideal model systems for the study of electron-transfer reactions would limit both the distance and the orientation of the donor and the acceptor in a controlled fashion.

One approach to this problem has been to covalently link aromatic electron acceptors such as pyrene with electron donors such as *N,N*-dimethylaniline. The link constrains the donor and acceptor to a limited range of distances and orientations. A large quantity of information has been obtained by studying such molecules.[1-3] Since these singly linked donor–acceptor pairs still possess a large degree of conformational freedom, measurements of their physical properties yield at best average values. Some of these problems have been eliminated by the use of multiple linkages. For example, doubly linked cofacial porphyrins have been examined.[4]

In this paper we present results concerning the electron-transfer properties of a chlorophyllide–pheophorbide cyclophane, Figure 1, in which the chlorophyll donor is strongly restricted in both distance and orientation relative to the pheophytin acceptor. This is accomplished by joining the two macrocycles with two covalent linkages.[5] This molecule may be viewed as a model of the primary electron donor–electron acceptor pair in green plant photosystem II. In photosystem II there is evidence that the primary donor may be a monomeric chlorophyll molecule, while the primary acceptor may be a monomeric pheophytin molecule.[6] This paper focuses on evidence for light-induced electron transfer in the chlorophyllide–pheophorbide cyclophane model for photosystem II.

Experimental Section

The cyclophane was prepared as described earlier.[5] A final purification was performed by HPLC.[7] The solvents used were reagent grade or spectral grade. Butyronitrile was purified as described earlier.[7] The solvents were deoxygenated by bubbling with dry nitrogen prior to dissolution of the cyclophane. In each case the solvents contained 1% pyridine in order to ensure that the single Mg atom was predominately pentacoordinate. Each solution was then transferred to a 1- or 2-mm path length cuvette for the optical studies.

Fluorescence decays were detected with a Hamamatsu streak camera equipped with an S-20 photocathode. A 30-μm slit was employed in all experiments except the wavelength dependence studies, where light limitations made it necessary to use a 100 μm slit. The time base of the streak camera most frequently used was 1.5 mm/ns (10 ps resolution), which displayed less than 5% nonlinearity when calibrated with an etalon. For the wavelength dependence studies a 0.25-m monochrometer (Jarrell-Ash) was placed after the sample. After collection and collimation of the light with a 50-mm focal length lens, a pair of 100-mm focal length achromatic lenses were used to direct the fluorescence through the monochromator and recollimate it. A 75-mm focal-length cylindrical lens was then used to image the fluorescence on the streak camera slit. Since the monochromator had a 2-mm output slit, the bandwidth of the fluorescence collected was 6 nm. Two color filters (Corning 3-66) and a spatial filter were used to block the laser excitation light.

[†] University of Illinois.
[‡] Argonne National Laboratory.
[§] Present address: Exxon Research and Engineering Co., Linden, NJ 07036.
[⊥] Alfred P. Sloan Fellow.

(1) N. Mataga and M. Ottolenghi in "Molecular Associations", Vol. 2, Z. Foster, Ed., Academic Press, New York, 1979, p 1.
(2) M. Gordon and W. R. Ware, Eds., "The Exciplex", Academic Press, New York, 1975.
(3) R. R. Bucks, T. L. Netzel, I. Fujita, and S. G. Boxer, *J. Phys. Chem.*, **86**, 1947 (1982).
(4) T. L. Netzel, P. Kroger, C. K. Chang, I. Fujita, and J. Fajer, *Chem. Phys. Lett*, **67**, 223 (1979).
(5) M. R. Wasielewski, W. A. Svec, and B. T. Cope, *J. Am. Chem Soc.*, **100**, 1961 (1978).
(6) I. Fujita, M. S. Davis, and J. Fajer, *J. Am. Chem. Soc.*, **100**, 6280 (1978).
(7) R. E. Overfield, A. Scherz, K. J. Kaufmann, and M. R. Wasielewski, *J. Am. Chem. Soc.*, **105**, 4256 (1983).

0002-7863/83/1505-5747$01.50/0

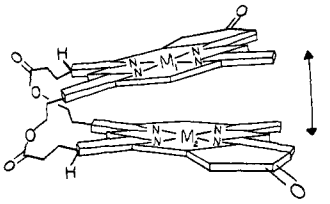

Figure 1. Structure of the chlorophyllide–pheophorbide cyclophane: M_1 = Mg and M_2 = H.

Temperature dependence studies were carried out by using a stainless-steel Dewar. The sample, in a 2-mm cuvette, was attached to a cold finger connected to the Dewar reservoir. The space surrounding the sample cell was evacuated. Filling the Dewar reservoir with liquid nitrogen resulted in a stable 97 K sample temperature. Intermediate temperatures were obtained by flowing a controlled stream of cold nitrogen into the reservoir. A feedback circuit controlling the cold nitrogen flow allowed temperature control to within 1 K.

The absorbance kinetics were obtained in a point by point fashion. White light continuum probe pulses of 10-ps duration were generated by pumping a 10-cm cell containing CCl_4 with 530-nm laser pulses. Each probe pulse was normalized for variations in the intensity of the continuum light by splitting off part of the light in a dual-beam arrangement. Kinetics were determined by changing the arrival time of the 530-nm exciting light with respect to the probe pulse with an optical delay line. The detector was a SIT vidicon (RCA). The vidicon output was digitized by an optical multichannel analyzer that was described earlier.[8] A Nova 3 minicomputer (Data General) was used for data collection and signal averaging. Data were transferred to a VAX 11/780 (DEC) for exponential analysis and graphics.

Elimination of stray fluorescence was crucial in obtaining absorption kinetics in the red absorbance band of the cyclophane. Probe light was focused with a 50-cm focal length lens onto a 1-mm aperture positioned 3 cm behind the sample and then refocused onto the entrance slit of a 1-m monochromator (Jarrell-Ash). This arrangement allowed only a very small solid angle of fluorescence to reach the detector. Additional fluorescence could be attentuated by placing neutral density filters after the sample. The contribution of fluorescence to the measured optical density change was determined by adjusting the optical delay line until the probe pulse reached the sample before the excitation pulse. The fluorescence artifact was less than the uncertainty of the absorbance measurement, i.e., 0.01 A.

Results

Fluorescence decay curves of the cyclophane are shown in Figure 2. The fluorescence decays were analyzed by the automatic Fourier transform program of Provencher.[9] The best fit in polar solvents is generally of the form

$$I = I_1 \exp(-t/\tau_1) + I_2 \exp(-t/\tau_2) \quad (1)$$

These fits show a signal to noise ratio of about 40 and are shown in Figure 2. Second best fits are single exponential decays. Biphasic fluorescence decays can arise from nonlinearity in the streak camera or from impurities in the sample. The linearity of the streak camera was checked by measuring the decay of methyl mesopyropheophorbide a in butyronitrile containing 25% iodoethane. In this medium the fluorescence lifetime of this compound is shortened by enhanced intersystem crossing due to the heavy-atom effect. The fluorescence decays exponentially with a 1.1-ns decay constant. Impurities are more problematic, since the monometalated cyclophane is somewhat unstable toward loss of its magnesium atom. Contributions from impurities, principally the metal-free cyclophane, were controlled by purifying the sample immediately before use. Any residual impurities were estimated by measuring the fluorescence decay of the same sample in different solvents. It is possible that some of the slow fluorescence decay component is due to the metal-free cyclophane. We estimate that this impurity contributes no more than 15% to the total fluorescence signal.

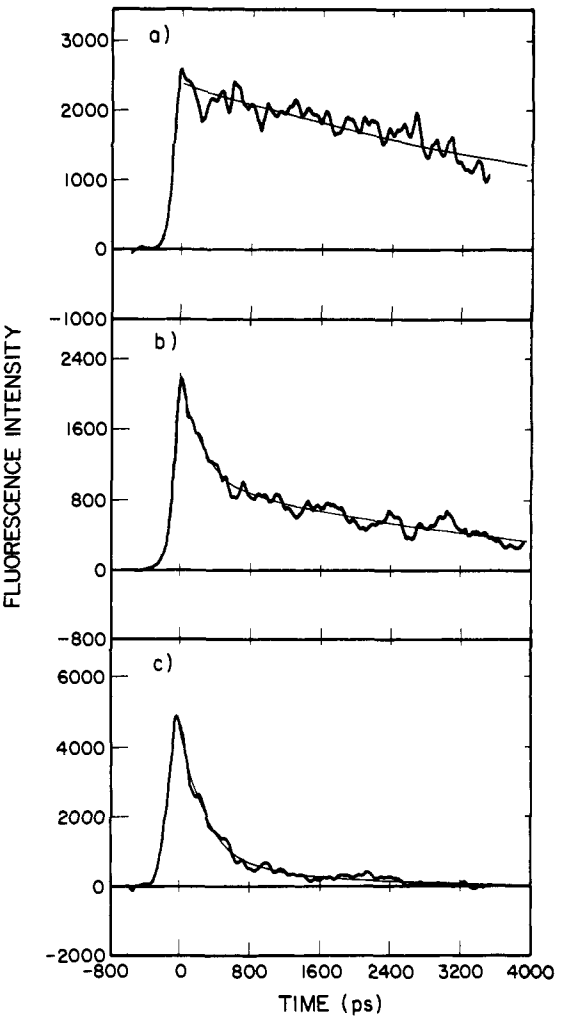

Figure 2. Fluorescence decay of 5×10^{-5} M monometalated cyclophane in (a) toluene, (b) dichloromethane, and (c) butyronitrile. The cell path length was 1 mm. The smooth line through the data is the best fit of eq 1 to the data.

Table I

solvent	dielectric const	slow/total fluorescence	fast decay const, ps	single exp decay const, ps
toluene	2.4	1.0		5905
chloroform	4.8	0.80	225	4274
iodoethane	7	0.21	231	
dichloromethane	9	0.49	229	1510
tert-butyl alcohol	11	0.56	474	1175
pyridine	12	0.30	274	396
butyronitrile	20	0.15	294	403
acetone	21	0.17	295	399
ethanol	24	0.18	312	372
methanol	33	0.12	175	365
dimethylformamide	35	0.14	247	287
formamide	109	0.39	226	2027
N-methylformamide	181	0.81	150	

The fast decay constant, τ_1 for the cyclophane in a variety of solvents, as well as the ratio of slow component to total fluorescence, $I_2/(I_2 + I_1)$, are presented in Table I. This table includes data for the solvent iodoethane, which gives an heavy-atom effect. The data in Table I show that the value of the fast decay constant remains about 250 ps more or less independent of solvent. The decay time constant of the slow component shows similar solvent invariance. The values of the slow decay component are uncertain by 50% due to the fact that data to only one time constant are available. They are in the range of 2–4 ns. The ratio of slow decay component to total fluorescence decreases as the dielectric constant

(8) K. K. Smith, C. J. Hawley, and K. J. Kaufmann, *SPIE*, **148**, 124 (1978).
(9) S. W. Provencher, *J. Chem. Phys.*, **64**, 2772, (1976).
(10) R. Haberkorn and M. E. Michel-Beyerle, *Biophys. J.*, **26**, 489 (1979).

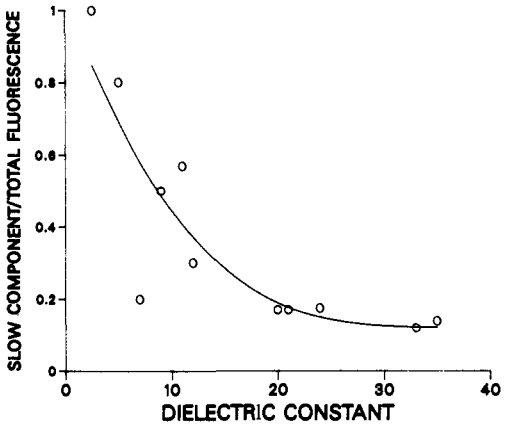

Figure 3. The ratio of slow fluorescence decay component to the total fluorescence from the monometalated cyclophane as a function of the solvent dielectric constant.

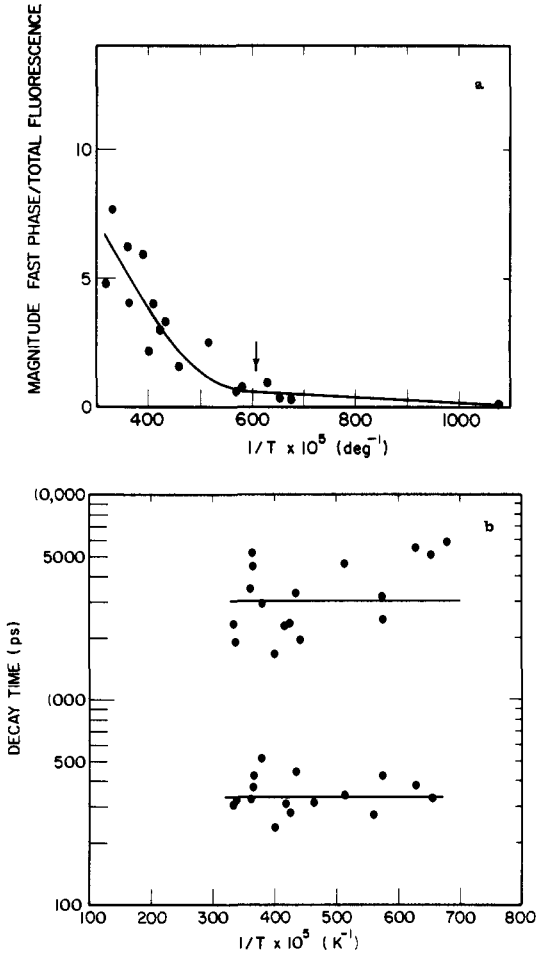

Figure 4. (a) The temperature dependence of the ratio of the fast fluorescence decay component to the total fluorescence from the monometalated cyclophane in butyronitrile. The arrow represents the freezing point of the solvent. (b) The temperature dependence of the two decay times of the monometalated cyclophane in butyronitrile (see eq 1). Concentration of the cyclophane was 1×10^{-4} M and the cell path length was 2 mm.

of the solvent increases. This behavior is summarized in Figure 3. Fluorescence lifetimes determined from the single exponential fits to the data also decrease as the dielectric constant of the solvent increases. The single exponential fits are also found in Table I.

The dependence of the fluorescence decay of the cyclophane in butyronitrile on emission wavelength was measured. The decay curves are wavelength independent within the experimental error of the measurement and are similiar to that illustrated in Figure 2c.

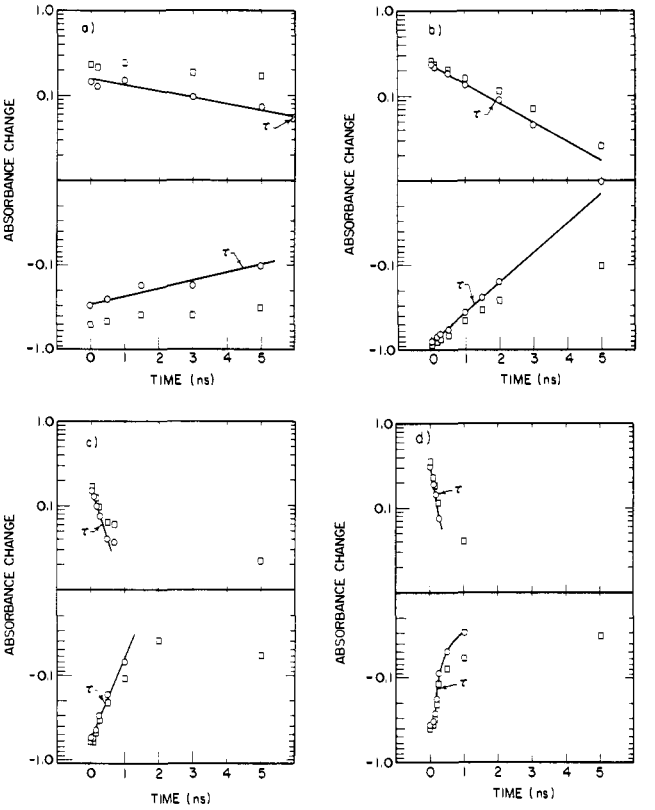

Figure 5. The decay of the negative absorption change at 655 nm and the positive absorption change at 445 nm. The squares represent the raw data, while the circles are the data corrected from residual long lived triplet absorbance. Data in four solvents are presented: (a) toluene, (b) dichloromethane, (c) butyronitrile, and (d) *N*,*N*-dimethylformamide.

The temperature dependence of the fluorescence decay of the cyclophane in butyronitrile is shown in Figure 4. As the temperature is lowered, the amount of the fast fluorescence decay component decreases, Figure 4a. The decay constants remain unchanged as the temperature decreases to the freezing point of the solvent. This is shown in Figure 4b. Below the freezing point of the solvent the fluorescence becomes monophasic and long-lived (>4 ns). Upon cooling the cyclophane in butyronitrile the red absorbance peak gradually shifts from 654 to 650 nm and sharpens from 17 to 11 nm full width at half height. This behavior is similar to that which is observed for the corresponding monomeric methyl mesopyrochlorophyllide a and monomeric methyl mesopyropheophorbide a. The failure to observe the formation of any absorbance to the red of 656 nm as the temperature is lowered indicates that aggregates did not form even at 97 K.

The transient absorbance changes of the excited cyclophane were also measured. Decay of the bleaching of the red-most band is particularly interesting, since bleaching of this band is generally diagnostic for the presence of lowest excited singlet and triplet states in addition to radical ion pair states.[7] The decay kinetics of both the bleaching at 655 nm and the positive absorbance change at 445 nm are presented in Figure 5. A long-lived component contributes between 10% and 50% of the total signal. This component is believed to be a triplet state of the molecule. The decay kinetics corrected for the residual triplet absorbance are also plotted in Figure 5. The corrected absorbance measures the repopulation of the ground state via all pathways other than slow intersystem crossing. The corrected decay constant at 445 nm agrees with that measured at 655 nm in each solvent to within 20%.

As the dielectric constant of the solvent increases, the lifetime for repopulation of the ground state shortens. Thus, while the measured lifetime at 445 nm in toluene is 5.5 ns, lifetimes of 1.9 ns and 420 ps are found in dichloromethane and butyronitrile, respectively. Similarly, lifetimes measured at 655 nm are 4.5 ns, 1.3 ns, and 450 ps in toluene, dichloromethane, and butyronitrile,

respectively. All absorbance measurements are best fit by single exponential decays. As the dielectric constant of the solvent is further increased, e.g., using *N,N*-dimethylformamide as the solvent, the absorbance change lifetime shortens to 230 ps. This decay shows significant nonlinear behavior on a semilog plot, Figure 5d.

Discussion

As the dielectric constant of the solvent is increased, the fluorescence and triplet yields of the cyclophane decrease.[7] It is therefore apparent that a new pathway is quenching the singlet state emission in higher dielectric constant solvents. The fact that the measured absorbance decays, Figure 4, are longer than the initial fluorescence decay, Figure 2, in these solvents indicates that another excited state is formed. The dielectric constant dependence suggests that this state possesses charge-transfer character.

The state that provides this nonradiative pathway out of S_1 does not itself emit. The radiative rate of the monometalated cyclophane is not a function of solvent dielectric constant and is similar in value to that for the dimetalated and non-metalated cyclophanes.[7] Also, the Stokes shift of the cyclophane is small and the wavelength maximum of its fluorescence is not substantially red shifted when the Mg in the cyclophane is pentacoordinate.[7] We therefore propose that transient formation of a short-lived radical ion pair is responsible for the observed fluorescence quenching. The possibility of spin dephasing yielding a triplet radical pair has not been addressed. Direct involvement of a triplet state in the early photochemistry is ruled out by the positive absorbance change in the region of 600–620 nm,[7] where the triplet state of chlorophyll shows a negative differential absorbance.[11]

To explain the biphasic fluorescence decay, we might hypothesize two ground-state configurations for the cyclophane. We might then suppose that one form can undergo electron transfer leading to decreased fluorescence lifetime while the other cannot. The ratio of the fast fluorescence component to the total fluorescence would then represent the equilibrium between two configurations. This scheme would require the absorbance changes to decay with the same lifetime as the fluorescence. However, the absorbance decay in dichloromethane is a single exponential with a time constant of 1.6 ns, Figure 5b. The initial fluorescence decay of the same sample is 230 ps. In butyronitrile most of the fluorescence decays in 300 ps, Figure 2b, but the absorbance change decays in 435 ps, Figure 5c. These observations rule out any dual ground-state configuration scheme and make it necessary to postulate the involvement of a dark excited state which is coupled to the emissive singlet state.

The net rate through the electron-transfer channel is on the order of 10^9 s^{-1} based on the measurements of fluorescence and triplet yield which are 0.04 and 0.01, respectively for the cyclophane in butyronitrile.[7] Since dielectric relaxation occurs on the order of 10 ps, it is not a rate-limiting step for electron transfer. Therefore, the fast fluorescence decay component represents the transition from the lowest excited singlet state to a radical ion pair state and thus reports the electron-transfer rate. The slow phase of the fluorescence decay indicates that the radical ion pair state can back react to the singlet state, which then emits.

The absorbance changes in Figure 5 measure excited singlet, triplet, and radical ion pair states. If the radical ion pair state were stabilized for long times, it would manifest itself as a long-lived absorbance change. However, the long-lived change in Figure 5 is readily accounted for by the triplet state based on triplet yield data.[7] The decay of the absorbance change therefore indicates that the radical ion pair returns to the ground state in <1 ns.

Figure 6 illustrates a kinetic model which accounts for the data. This kinetic scheme has a closed form solution identical in form with the one for excited-state proton-transfer reactions.[12] The rate constants in solvents with a variety of dielectric constants that best fit the data are given in Table II. These rate constants account for the kinetics of the biphasic fluorescence decay, the absorbance decay, and the fluorescence and triplet yields.

Table II

Solvent-Independent Rate Constants

$k_F = 3 \times 10^7$ s^{-1}

$k_{ISC} = 3 \times 10^7$ s^{-1}

$k_P = 1 \times 10^3$ s^{-1}

Solvent-Dependent Rate Constants

solvent	$10^{-9}k_{ET}$, s^{-1}	$10^{-9}k_{ETB}$, s^{-1}	$10^{-9}k_{NR}$, s^{-1}
dichloromethane	2	1	1
butyronitrile	3	≤ 1	3
N,N-dimethylformamide	4	≤ 1	2

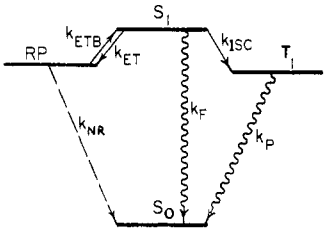

Figure 6. This state diagram models both the decay kinetics and the quantum yield information which were measured for the cyclophane. The states shown are S_0, the ground singlet state, S_1, the lowest excited singlet state, T_1, the lowest excited triplet state, and RP, the radical ion pair state. The transitions between the states are also shown. S_1 may decay to T_1 via intersystem crossing, k_{ISC}, to the ground state by emission, k_F, and to RP by electron transfer, k_{ET}. RP may back react to S_1, k_{ETB}, or undergo nonradiative internal conversion to S_0, k_{NR}. T_1 slowly returns to S_0 by phosphorescence or internal conversion, k_P.

It is difficult to be absolutely certain of the completeness of the kinetic model. Nevertheless, it is the simplest model that accounts for all the data. The kinetic scheme in Figure 6 is equally valid if the single exponential fits to the fluorescence decays are used. In that case the fluorescence decay still monitors the rate of electron transfer from the first excited singlet state of the molecule, k_{ET}, while the rate of radical ion pair recombination, $k_{ETB} = 0$. In either case electron transfer in this donor–acceptor system is relatively slow with an upper limit of 4×10^9 s^{-1}.

The absence of a fast fluorescence decay component in toluene indicates that the monometalated cyclophane does not undergo electron transfer in this solvent. The dimetalated cyclophane exhibits a shortened fluorescence decay constant only in butyronitrile, while the nonmetalated cyclophane does not show a fast fluorescence decay component in any of the solvents tested.[7] These observations may be accounted for by the energetic requirement for electron transfer.

The energy needed to transfer an electron from a donor to an acceptor is provided by the excitation photon but can be no greater than the energy of the lowest excited singlet state because relaxation within the singlet manifold is rapid. This excitation must provide the energy needed to oxidize the donor and to reduce the acceptor

$$U^{\pm} = W^* - E_d^+ + E_a^- + V \qquad (2)$$

Additional work is required to separate the charge. This is represented by the term V in eq 2. Other terms are given in Table III. The energy required to bring two ions of charge q_i and q_j together to separation R from infinite separation is given by the Onsager equation.[12]

$$V = -\left(\frac{\epsilon - 1}{2\epsilon + 1}\right)D^2/a^3 + q_iq_j/R + \left(\frac{\epsilon - 1}{\epsilon}\right)(q_i^2/2r_i + q_j^2/2r_j) \qquad (3)$$

(11) K. Siefert and H. T. Witt, *Naturwissenschaften*, **55**, 222 (1968).

(12) J. E. Ireland and P. A. H. Wyatt, *Adv. Phys. Org. Chem.*, **12**, 131 (1976).

(13) L. Onsager, *J. Am. Chem. Soc.* **58**, 1486 (1936).

Table III. Energetics for Electron Transfer (in eV)

	E_d^+	E_a^-	W^*
methyl mesopyrochlorphyllide a (MPChl)	+0.54	−1.3	1.90
methyl mesopyropheophorbide a (MPPh)	+0.85	−1.07	1.89

$U^{\pm}$ = excess free energy of electron transfer
W^* = singlet excited state energy
E_d^+ is the oxidation potential of the donor (vs. SCE)
E_a^- is the reduction potential of the acceptor (vs. SCE)
V is the electrostatic term (see text)

	$U^{\pm}$ (oxidation-reduction terms only)
$MPChl^+$-$MPChl^-$	0.06
$MPChl^+$-$MPPh^-$	0.28
$MPPh^+$-$MPPh^-$	−0.03

	dielectric constant					
	2.4	4.8	9.0	12.3	20.0	24.8
	$U^{\pm}$ (Onsager reaction field)					
Chl-Chl	−1.15	−0.43	−0.12	−0.03	0.06	0.09
Chl-Ph	−0.93	−0.21	0.10	0.19	0.28	0.31
Ph-Ph	−1.24	−0.52	−0.21	−0.12	−0.03	0.00
	$U^{\pm}$ (Weller formula)					
Chl-Chl	−0.27	−0.19	−0.15	−0.13	−0.11	−0.11
Chl-Ph	−0.05	0.02	0.08	0.09	0.10	0.10
Ph-Ph	−0.36	−0.28	−0.24	−0.22	−0.20	−0.20

Here r_i and r_j are the ionic radii, a is the radius of the cavity within the material possessing dielectric constant ϵ in which the dipole lies, and D is the dipole moment. Table III summarizes the free energies involved. The oxidation and reduction potentials of methyl mesopyrochlorphyllide a and methyl mesopyropheophorbide a have been determined.[14] The convention used in Table III is that of Seeley.[15] In this convention the reaction is allowed if the quantity U is positive. The Onsager model fits the data only in the unrealistic case when a cavity radius of 0.385 nm and ionic radii of 0.5 nm are used. Calculations with larger cavity radii predict that the cyclophanes containing zero, one, or two Mg atoms could all undergo electron transfer even in solvents having low dielectric constants.

The difficulty with the above approach is that it requires a number of assumptions in calculating the solvation energy of the ions that are unrealistic for large molecular ions. Another approach to the calculation of the energy of the ion pair is to use the empirical formulas developed by Weller and his associates[2,13] to calculate the formation energy of exciplexes.

$$V = D^2/a^3\left(\frac{\epsilon - 1}{2\epsilon + 1}\right) - (U_{dest} - U_{stab}) - 0.52 \text{ eV} \quad (4)$$

The terms U_{dest} and U_{stab} are energy terms that arise from the interaction of the exciplex charge-transfer state with the ground and lowest excited singlet states both of the donor and of the acceptor. We have taken these terms to be zero because we find no evidence for exciplex emission. The absence of large wavelength shifts in the absorption spectrum of the cyclophane relative to that of its monomeric constituent molecules indicates that at most a weak coupling exists between the radical ion pair state and the other states of the donor and of the acceptor. A value for D^2/a^3 of 0.75 ± 0.3 eV was empirically found to fit a large selection of data by the Weller group. This number is used in the calculations that are found in Table III. These results fit the experimental trends quite well.

Comparison of Figure 4 with Figure 3 and the data in Table I show that the fluorescence kinetics are affected in similar ways by increasing the solvent dielectric constant or by increasing the temperature. At low temperatures dielectric relaxation occurs only by the polarizability of the solvent, since dipole rotations are frozen out. Below the freezing point of butyronitrile, indicated by an arrow in Figure 4a, the fluorescence decay of the cyclophane consists entirely of a slow component, indicating that electron transfer cannot occur.

The effect of temperature on the electron-transfer process could therefore arise from the inabililty of the solvent to relax and thereby stabilize the ion pair. Alternatively, a new conformation of the molecule which cannot undergo electron transfer from the singlet state could be formed at low temperature. Low-temperature ground-state spectra do not reveal the presence of another conformation. However, since temperature-dependent absorbance kinetic studies were not carried out, this possibility cannot be ruled out.

The very "slow" formation of the charge separation in the cyclophane contrasts with that of the cofacial porphyrin dimer containing one metalloporphyrin and a free base porphyrin. Electron transfer within these cofacial porphyrins is reported to occur in <6 ps, and the resultant radical ion pair is reported to possess a 600-ps lifetime.[4] The distance between the donor and the acceptor chromophores in the cyclophanes and the cofacial porphyrin is similar. The major difference between these two systems is the degree of symmetry and the rigidity of their structures. The cofacial porphyrin exhibits C_{2h} symmetry and a strong exciton interaction between the chromophores. This interaction manifests itself in a 25-nm blue shift of the porphyrin Soret band.[16] On the other hand the chlorophyllide–pheophorbide cyclophane consists of two chlorins that have discrete $Q(0,0)$ transitions in the plane of each macrocycle. In each macrocycle of the cyclophane the $Q_y(0,0)$ transition is oriented along the ring I–ring III axis. In the cyclophane the $Q_y(0,0)$ transition of one macrocycle is perpendicular to that of its partner macrocycle. This geometry results in only weak vibronic coupling between the macrocycles in the cyclophane.[7] This weak coupling may be responsible for the relatively slow intramolecular electron-transfer rate observed.

The two chains linking the macrocycles of the cyclophane allow a jawing motion to take place within the molecule in a manner suggested in Figure 1. This is the principal translational degree of freedom that the two macrocycles possess relative to one another. The linkages of the cofacial porphyrin allow only slippage of one macrocycle across the face of its partner to occur. This more subtle difference in geometry between two molecules that to a first approximation possess a relatively high degree of motional constraint between the donor and the acceptor may also play a crucial role in determining the rate of electron transfer. These models point out the importance of donor–acceptor geometry because the distances between the donor and the acceptor in each case are very similar. Eisenthal and co-workers came to a similar conclusion in their study of the electron-transfer reaction between the excited singlet state of anthracene and *N,N*-dimethylaniline.[17] This reaction is very rapid at room temperature, about 1.6×10^{10}, but is completely blocked as the temperature is lowered. Eisenthal interpreted this drastic change in the rate as due to the need for the donor and acceptor to properly orient before the reaction could take place.

The electron-transfer properties of the cyclophane suggest several points regarding photosynthetic reaction center structure especially as regards photosystem II of green plants. First, close proximity between the chlorophyll *a* donor and the pheophytin *a* acceptor do not necessarily ensure forward electron-transfer rates approaching the in vivo rate of about 10^{12} s^{-1}. The cyclophane data show that there exist geometries for which this rate is as slow as 4×10^9 s^{-1}. Second, the charge separation in the model system collapses in about 1 ns. This is about 10 times faster than the back electron transfer in vivo. This implies that either the donor–acceptor geometry is not optimum or there is a need for an intermediary acceptor (or donor) in order to achieve slower back reaction rates as has been proposed for the photosynthetic bacterium Rhodopseudomonas sphaeroides.[18] Third, the absence

(14) M. R. Wasielewski, unpublished data.
(15) G. R. Seeley, *Photochem. Photobiol.*, **27**, 639 (1978).
(16) C. K. Chang, *Adv. Chem. Ser.*, No. **173**, 162 (1979).
(17) T. J. Chang and K. B. Eisenthal, *J. Chem. Phys.*, **62**, 2213 (1975).

of charge separation at low temperature, where dielectric relaxation can no longer stabilize the radical ion pair, suggests that charged functional groups are important in stabilizing photosynthetic charge separation in vivo. In photosynthetic organisms charge separation proceeds efficiently even at cryogenic temperatures. Model donor-acceptor systems with good distance and geometry constraints need to incorporate charged groups to better simulate the natural environment of photosynthetic reaction centers.

Acknowledgment. We wish to thank Peter Rentzepis, Danny Huppert, and Steve Milton for helping us with some of the fluorescence measurements. This work was sponsored by the Division of Chemical Sciences, Office of Basic Energy Sciences, of the Department of Energy. We wish to thank the National Science Foundation for providing the VAX 11/780 at the University of Illinois.

Registry No. Chlorophyllide-pheophorbide cyclophane, 86563-02-2.

(18) D. Holten, C. Hoganson, M. W. Windsor, C. C. Schenck, W. W. Parson, A. Migus, R. L. Fork, and C. V. Shank, *Biochim. Biophys. Acta*, **592**, 461 (1980).

Optical Absorption, Electron Spin Resonance, and Electron Spin Echo Studies of the Photoionization of Tetramethylbenzidine in Cationic and Anionic Synthetic Vesicles: Comparison with Analogous Micellar Systems

A. S. W. Li† and Larry Kevan*

Contribution from the Department of Chemistry, University of Houston, Houston, Texas 77004.
Received February 10, 1983

Abstract: The photoionization of *N,N,N',N'*-tetramethylbenzidine (TMB) in dihexadecylphosphate anionic vesicles and in dioctadecyldimethylammonium chloride cationic vesicles has been studied by optical absorption and electron spin resonance in liquid and frozen solutions. The TMB cation has been observed to be stabilized in both types of vesicles. The photoionization efficiency is about twofold greater in the cationic vesicles compared to the anionic vesicles. Shifts in the optical absorption maximum between micellar and vesicle solutions indicate that TMB is in a less polar environment in the vesicle systems. Electron spin echo modulation spectrometry has been used to detect TMB cation-water interactions that are found to be weaker than in previously studied micellar solutions. This is consistent with the optical absorption results and with an asymmetric solubilization site for TMB and TMB^+ within the vesicular structure. A new absorption in the photoionized vesicles is assigned to a nonparamagnetic diamine-diimine charge-transfer complex between two TMB cations in the same vesicle. This complex is not formed in micellar systems.

Photoinduced charge separation and photosensitized electron transport in organized molecular assemblies such as micelles and vesicles are being widely studied as models for artificial photosynthetic systems.[1-6] To optimize the charge separation efficiency in such systems, it is necessary to understand the role of the geometry and structural location of the photoactive molecule in the organized molecular assembly. We have recently shown how electron spin resonance (ESR) and electron spin echo modulation (ESEM) can be successfully used to deduce the surrounding structure of paramagnetic species in frozen solutions.[7,8] Most recently we have shown how ESR and ESEM can be used to obtain structural information about photoproduced aromatic amine cations in micellar systems.[9,10] In this work we extend such investigations to studies of photoproduced cations in synthetic cationic and anionic vesicle systems. We find interesting contrasts with micellar systems that give new information about the structural requirements for optimum photogenerated charge separation in organized molecular assemblies.

Experimental Section

The anionic surfactant dihexadecylphosphate (DHP) was obtained from Sigma Chemicals, the cationic surfactant dioctadecyldimethylammonium bromide (DODAB), and the aromatic amine *N,N,N',N'*-tetramethylbenzidine (TMB) were obtained from Eastman Chemicals. DHP and DODAB were purified by recrystallization from acetone. DODAB was exchanged by chloride ion to produce dioctadecyldimethylammonium chloride (DODAC).[11] This was done by passing a solution of DODAB in MeOH-$CHCl_3$ (70:30, v/v) solvent through a polystyrene exchange resin type AG2-X8 from Bio-Rad Laboratories. The DODAC was purified by recrystallization from acetone/water mixtures (95/5 volume ratio).

The vesicle solutions were prepared by dissolving the synthetic surfactants in triply distilled water (over alkaline permanganate and acid dichromate) heated to 80 °C followed by sonication with a Fisher Model 300 sonic dismembrator operated at 30 W with a 4-mm o.d. microtip for 1 h at 80 °C. The initial aqueous solution is a cloudy suspension, but after sonication it becomes a clear solution with a slight bluish color. Typical concentrations used are 9 mg of DODAC, 6 mg of DODAB, and 6 mg of DHP, each in 1.5 mL of water. For some of the electron spin

† Present address: Department of Chemistry, University of Petroleum and Minerals, Dhahra, Saudi Arabia.

(1) Calvin, M. *Acc. Chem. Res.* **1978**, *11*, 369.
(2) Grätzel, M. *Ber. Bunsenges. Phys. Chem.* **1980**, *84*, 981.
(3) Fendler, J. H. *J. Phys. Chem.* **1980**, *84*, 1485; *Acc. Chem. Res.* **1980**, *13*, 7.
(4) Thomas, J. K. *Acc. Chem. Res.* **1977**, *10*, 133.
(5) Atik, S. S.; Thomas, J. K. *J. Am. Chem. Soc.* **1981**, *103*, 4367.
(6) Tunuli, M.; Fendler, J. H. *J. Am. Chem. Soc.* **1981**, *103*, 2507.
(7) (a) Kevan, L. *Acc. Chem. Res.* **1981**, *14*, 138. (b) Kevan, L. *J. Phys. Chem.* **1981**, *85*, 1628.
(8) (a) Ichikawa, T.; Kevan, L. *J. Chem. Phys.* **1980**, *72*, 2295. (b) Ichikawa, T.; Kevan, L. *J. Phys. Chem.* **1980**, *84*, 1955. (c) Narayana, M.; Kevan, L. *J. Am. Chem. Soc.* **1981**, *103*, 1618. (d) Janakiraman, R.; Kevan, L. *J. Chem. Phys.* **1981**, *75*, 1658. (e) Ichikawa, T.; Kevan, L. *J. Am. Chem. Soc.* **1982**, *104*, 1481. (f) Narayana, P. A.; Kevan, L. *J. Magn. Reson.* **1982**, *46*, 84. (g) Narayana, P. A.; Suryanarayana, D.; Kevan, L. *J. Am. Chem. Soc.* **1982**, *104*, 3552. (h) Janakiraman, R.; Kevan, L. *J. Phys. Chem.* **1982**, *86*, 2727. (i) Narayana, P. A.; Suryanarayana, D.; Kevan, L. *Ibid.* **1982**, *86*, 2729.
(9) Narayana, P. A.; Li, A. S. W.; Kevan, L. *J. Am. Chem. Soc.* **1981**, *103*, 3603.
(10) Narayana, P. A.; Li, A. S. W.; Kevan, L. *J. Am. Chem. Soc.* **1982**, *104*, 6502.
(11) Lim, Y. Y.; Fendler, J. H. *J. Am. Chem. Soc.* **1979**, *101*, 4023.

0002-7863/83/1505-5752$01.50/0